System Characterization of a Novel Haptic Interface for Natural Orifice Translumenal Endoscopic Surgery Simulation

Saurabh Dargar-*IEEE Student Member*, Ganesh Sankaranarayanan, *IEEE Member*, and Suvranu De, *IEEE Senior Member*

***Abstract*— Natural orifice translumenal endoscopic surgery (NOTES) is a minimally invasive procedure, which utilizes the body's natural orifices to gain access to the peritoneal cavity. The VTEST© is a virtual reality NOTES simulator developed at the CeMSIM at RPI to train surgeons in NOTES. A novel 2 DOF decoupled haptic device was designed and built for this simulator. The haptic device can render 5.62 N and 190.05 N-mm of continuous force and torque respectively. In this work we have evaluated the haptic interface and developed a model to accurately describe the system behavior, to further incorporate into an impedance type controller for realistic haptic rendering in the VTEST©.**

I. Introduction

Minimization of patient trauma during a surgical procedure is always a factor of consideration. Post operative pain can be more frequently attributed to trauma due to surgical access rather than the final surgical task [1]. This ideology of access trauma minimization has driven the field of minimally invasive surgery (MIS) which employs new methodologies to gain access to the patients target organ. MIS endeavours led to the development of laparoscopy and now Natural Orifice Translumenal Endoscpic Surgery (NOTES). The NOTES procedure is designed to minimize external scarring and patient trauma [2], by gaining access to the target organ by breaching the lumen of the colon, cervix or stomach via the mouth, vagina or anus [3,4]. The potential benefits of NOTES are driving the surgical community to actively explore the technique, and multi-center clinical trials have been set in motion with some positive results already published [5,6].

A NOTES procedure is performed using one of two ways–pure or hybrid. In a pure NOTES procedure, a flexible endoscope is used to access the organs through a natural orifice. In a hybrid procedure an additional single laparoscopic port (usually through the navel) is used to access the organs with laparascopic tools with a rigid endoscope through the natural orifice [7]. The control and maneuvering of a flexible endoscope in pure NOTES requires critical scope handling skills to safely breach the respective lumen to gain access to the organ [8]. The tough nature of the procedure warrants the use of simulators for repeated training in simple and difficult scenarios. There are existing simulators for colonoscopy and other endoscopic procedures, however none for the NOTES procedure. Samur et al developed a 2 degree-of-freedom haptic device specifically for colonoscopy simulations with the ability to provide both active and passive translational force feedback to the user [9]. Yi et al. developed a 2 DOF colonoscopy simulator with a long and flexible tube with a custom sensor to measure the jiggling forces, which are unique to a colonoscopy procedure [10]. Ikuta et al designed a colonoscopy simulator called the Portable Virtual Endoscope System (Portable VES) [11]. There are also some commercial devices such as the EndoVR system from CAE Healthcare and the GI Mentor from Simbionix USA Corp [12,13,14]. At the Center of Modeling, Simulation and Imaging in Medicine (CeMSIM) at RPI, we have developed a virtual reality simulator for NOTES known as the VTEST© (Virtual Translumenal Endoscopic Skills Trainer). As part of this simulator we have developed a new haptic device with decoupled force feedback mechanisms for translational and rotational haptic feedback and have in this work shown the design and evaluation of the novel haptic hardware.

II. System components & Design

A. System Design

The VTEST© hardware interface has been designed to resemble a patient undergoing a NOTES transvaginal procedure. Hardware realism is an important factor in recreating a realistic surgical simulation and aids in the learning process. The VTEST© has been designed and built to resemble a patient while lying down on the operating table covered in surgical drapes. The silicone foam insufflated abdomen and silicone trans-vaginal entry port can be seen in the CAD design of the hardware interface in Fig. 1.

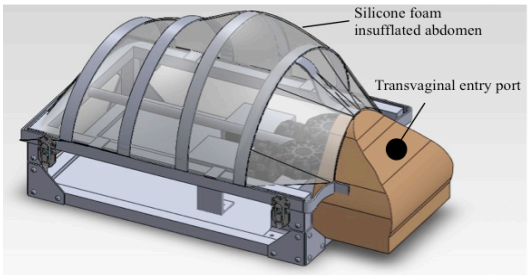

Figure 1. A CAD model of the VTEST© simulator with a soft silicone sheet covering the abdomen

Research funded by NIH, NIH/NIBIB 5R01EB010037-01, 1R01EB009362-01A2, 2R01EB005807- 05A1, 1R01EB014305-01A1

Saurabh Dargar is a graduate student in the Biomedical Engineering Department and with the Center for Modeling, Simulation and Imaging in Medicine at Rensselaer Polytechnic Institute in Troy, New York, USA (e-mail: dargas@rpi.edu).

Ganesh Sankaranarayanan is a Research Assistant Professor in the Department of Mechanical, Aerospace and Nuclear Engineering (MANE) and the Center for Modeling, Simulation and Imaging in Medicine (CeMSIM) at Rensselaer Polytechnic Institute in Troy, New York, USA (e-mail: sankag@rpi.edu).

Suvranu De is the Director of the Center for Modeling, Simulation and Imaging in Medicine (CeMSIM) and Head of the Department of Mechanical, Aerospace and Nuclear Engineering (MANE) at Rensselaer Polytechnic Institute in Troy, New York, USA (e-mail: des@rpi.edu).

Our hardware interface uses an actual flexible endoscope instrumented with high precision rotary encoders (CE300-40, MicroE Systems, Bedford, MA) to measure the manipulation of the flexible tip [15]. Using an actual endoscope provides realistic force feedback at the control knobs, a necessity for a realistic simulation of the procedure.

B. *The Haptic Interface*

The haptic hardware architecture responsible for rendering forces onto the flexible endoscope is found within the simulated patient abdomen, as shown in Fig. 2. The haptic device is a 2 degree-of-freedom force feedback device capable of providing translational and rotational force feedback to the user via the endoscope.

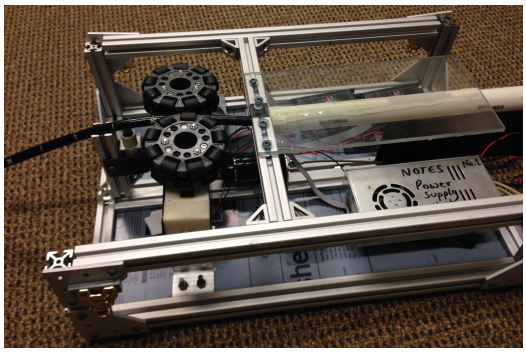

Figure 2. The Haptic Interface with the silicone foam abdomen cover removed to reveal the embedded actuation and control electronics

The endoscope is pre-inserted through the trans-vaginal entry port, where it interfaces with the two decoupled force feedback units. It is critical to decouple the 2 DOFs to allow full functionality of each of the DOFs without one interfering in the other's actuation capabilities. The translational force feedback unit uses two dual hub omni-directional friction rollers to grip the flexible endoscope and apply force for the user to feel (Fig. 3). The dual hub nature of the omni-direction rollers allows four points of contact with the endoscope at all times. There are 18 individual rubber rollers on each friction roller, which decouple the rotational and translation motion of the endoscope. Two RE40 DC motors (Maxon Motor, Switzerland) are directly coupled to the friction rollers which apply torque in a synchronized manner to minimize slip. The DC motors are placed within housings with high stiffness springs that apply a force on the motor towards the endoscope, further ensuring sufficient contact force on the endoscope. The translational force-feedback unit independently has an unlimited workspace, however it is limited to the length of the endoscope in use.

The rotational force feedback unit uses a 20 inch long flexible drive shaft to interface with the tip of the flexible endoscope. A RE40 brushless DC motor is connected to the other end of the flexible drive shaft, which transmits the torque to the flexible endoscope and eventually to the user's hand. This mechanism for rotational force feedback ensures an unlimited workspace; Fig. 4 shows the method of actuation.

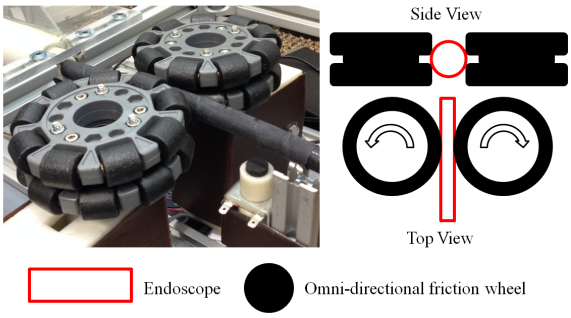

Figure 3. The translational force feedback unit with a schematic diagram of the method of force application

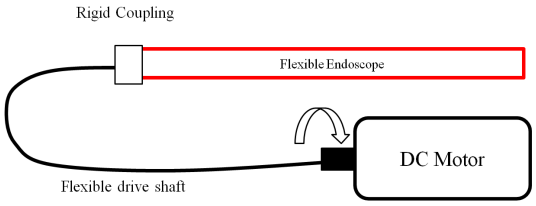

Figure 4. Schematic of the rotational force feedback mechanism

The DC motor's inbuilt rotary optical encoder is used to measure the endoscope's linear and angular orientation in real-time, which is then used in the virtual environment to simulate the endoscope's motion. The three DC motors in the haptic device are controlled by three separate servo controllers, which are interfaced with the simulation computer via a high speed DAQ (National Instruments NI-USB-6341).

III. System Characterization

The characterization of the system is the first step to being able to control the haptic device. Achieving system transparency by ensuring the transmission of the virtual environment impedance (Z_E) without any distortion, is the primary goal of system characterization for a haptic device. Multiple device performance parameters have been identified in literature through years of haptic device research, most notably the work of Ellis *et al* [16] from Queen's University at Kingston in Ontario, Canada and Hayward *et al* [17] at McGill University, Montreal, Canada. Specifically in this work, we have evaluated the static and frequency response of the 2-DOF haptic device in use for the VTEST©.

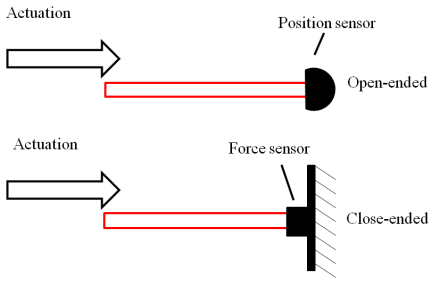

Figure 5. Schematics of the two boundary conditions used in the experiments.

We imposed two types of boundary conditions on our system during the course of the experiments, open-ended and

close-ended as shown in Fig. 5. The end effector (location of human grip on flexible endoscope) was instrumented with a position sensor in the open ended configuration. In the close ended configuration the end effector was arrested using a vice grip with a load cell between the end effector and vice-grip. We used a magnetic position tracking device as the position sensor (TrakStar, Ascension Technology Corporation, Shelburne, VT) and a 6-axis load cell as the force and torque sensor (ATI Industrial Automation, Apex, NC). Both these experimental conditions were imposed on both translational and rotational DOFs.

A. System Static Response

Studying the system static response was able to provide us the haptic device's maximum force output capabilities. Since our haptic device will mostly be used for continuous force output instead of an impulse like force, we are interested in maximum continuous force. The device was given a steady ramp up and ramp down force input in both DOFs while in the close-ended configuration, as the load cell recorded the force and torque. Fig. 6 and Fig. 7 show the results of the experiments for translational and rotational force feedback respectively. The maximum continuous translational force and rotational torque is 5.62 N and 190.05 N-mm respectively.

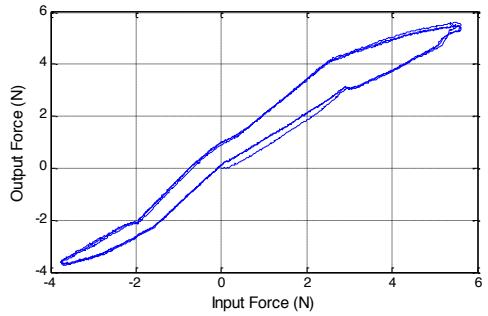

Figure 6. Input-Output curve of the translational degree of freedom. Motors were commanded a ramp-up and ramp-down input force (+6N to -4 N)

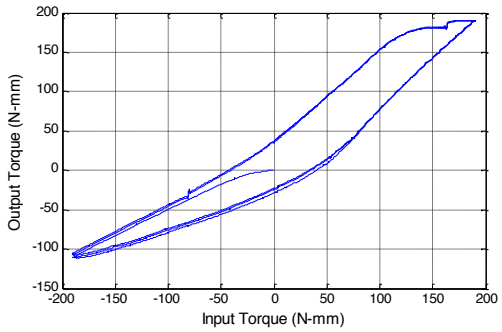

Figure 7. Input-Output curve of the rotational degree of freedom. Motors were commanded a ramp-up and ramp-down input torque of (+190 N-mm to -190 N-mm)

In both DOFs we notice nonlinearity in the input-output relationship, as the same input gives a different output when the direction of actuation changes. This hysteresis in the relationship can be attributed to friction in the system, which needs to be overcome by the device prior to being able to transmit any force to the user. Hence we can observe a loss in transmission in the input-output relationship. We also note that the rotational DOF has a dominant direction of force feedback. The clockwise (+ve) direction of rotational actuation has the best reproduction of torque while the counter-clockwise (-ve) direction sees a significant loss in transmission. This is due to the directional winding of the metal threads of the flexible shaft, and can be accounted for with a direction specific compensator in the control algorithm.

B. System Frequency Response

A frequency response analysis was performed on the device to be able to describe the system and determine the useful force bandwidth of the haptic system. In both configurations, the haptic device was excited with a 1-30 Hz chirp input signal and the output force and position data was recorded. The first open-ended experiment determined *V(s),* the relationship between input-force and output-velocity. The velocity was calculated by taking the derivative of the position data with respect to the sampling rate. The noise that is introduced to the system by taking the derivative was reduced by a 30 Hz lowpass Butterworth filter.

$$V(s) = \frac{V_{ee}}{F_{des}} \tag{1}$$

The second, close-ended experiment determined the input-force and output-force relationship, *F(s)*.

$$F(s) = \frac{F_{ee}}{F_{des}} \tag{2}$$

Where F_{ee} is the force measured at the end effector of the flexible endoscope and F_{des} is the desired output force as commanded by the input to the system. Using equation (3), the devices uncontrolled output impedance, Z_{device} was determined.

$$F(s) = Z_{device} \times V(s) \tag{3}$$

The relationships in equation (1) and (2) were used to estimate the transfer function from the collected experimental data. The transfer function estimations were performed using the greybox modeling method, a part of Matlab's system identification toolbox. The transfer function estimates were performed to fit the modified fourth order mass spring damper system dynamic model as shown in Fig. 8. The transfer function *V(s)* and *F(s)* in the context of the given dynamic model can be described as follows;

$$V(s) = 1/((M_m + M_s)\boldsymbol{s} + (b_s + b_m))$$

$$F(s) = \frac{k_s}{(M_m M_s)\boldsymbol{s^4} + (M_s(b_s + b_m) + M_m b_s)\boldsymbol{s^3} + (M_s k_s + M_m k_s + 2b_m b_s)\boldsymbol{s^2} + (b_m k_s)\boldsymbol{s}} \tag{4}$$

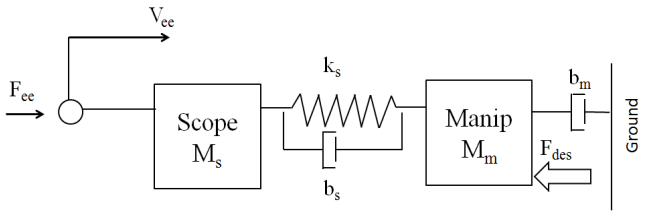

Figure 8. The 1 DOF 4th order modified mass-spring-damper dynamic system model (subscript s=scope, m=manipulator)

Fig. 9 and Fig. 10 shows the Bode plot of *F(s)* for the linear and rotational force feedback respectively. The plot compares the input force and output force relationship obtained from the experimental data against the estimated model. Both DOFs show that the response of the model deviates from the experimental data in the higher frequency range (above 10 Hz), however the model approximated the overall behavior fairly well. The calculated force bandwidth of the device was 18.1 Hz for the translational DOF and 5.7 Hz for the rotational DOF.

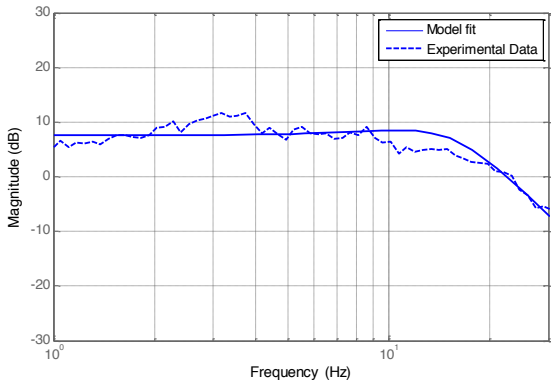

Figure 9. A Bode magnitude plot of *F(s)* for the translational DOF. A 4th order model was fit to the data to estimate the transfer function.

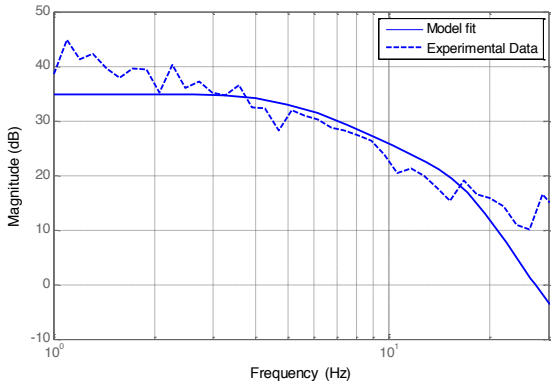

Figure 10. A Bode magnitude plot of *F(s)* for the rotational DOF. A 4th order model was fit to the data to estimate the transfer function

Using the estimations of the transfer functions in (4) as shown in Figure 9 and 10, the model for the device impedance was estimated by $Z_{device} = F(s)/V(s)$. Fig. 11 demonstrates the frequency response of the rotational DOF. Once again it is noted that the model performance declines beyond ~10 Hz. This is not a major concern since it has been shown that human hand interactions remain under 10 Hz, thus making our device capable of performing within the desired range [18,19]. A similar result was also seen for the impedance of the translational DOF. The overall system characteristics were obtained from the approximation of the system impedance transfer functions, and are shown in Table 1. The mass, stiffness and damping parameters shown in Table 1 are aggregate parameters, and are the sums of the different masses, spring and dampers in the dynamic model shown in Figure 8. These parameters are critical as they are the input parameters to the control algorithm for the closed loop impedance control as well as the friction compensation.

TABLE 1. THE APPROXIMATION OF THE 4TH ORDER DEVICE DYNAMICS

System Parameter	Rotational	Translational
Mass (Inertia/Mass)	0.00118 kg.m^2	0.2 kg
Stiffness (K)	1.008 Nm/rad	785 N/m
Damping (B)	0.0416 Nm.s/rad	9.2 Ns/m

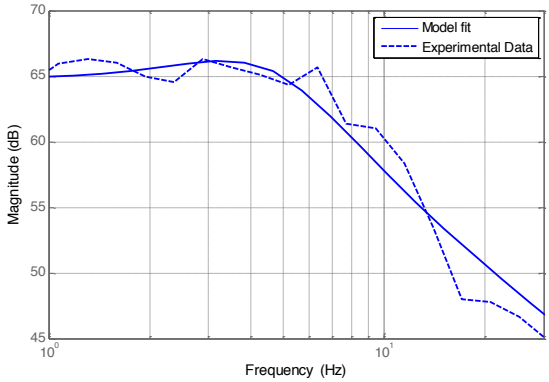

Figure 11. A Bode magnitude plot of $Z_{device}(s)$ for the rotational DOF. The comparison of the experimental data vs. the 4th order model fit highlights the operational frequency range.

IV. DISCUSSION

The multiple number and configurations of experiments performed on this device have allowed us to determine a variety of system defining parameters. The static response of the device illustrated the maximum continuous force and torque the device is capable of. A concurrent study performed here at CeMSIM, studied the haptic feedback surgeons felt during the course of a NOTES procedure on a porcine model. Data was colected for 10 surgeons and the range of force and torque applied by the user was measured, serving as a benchmark study for actuation. The mean max pull/push resistance in translation force was found to be 4.5 N/9.9N while the mean max CW/CCW torque resistance in rotation was 76.7 N-mm/85 N-mm for all 10 subjects [20]. The comparison of the haptic device's actuation capapbilites (max cont. force 5.62 N, max cont torque 190.05 N-mm) and the benchmarked capabilities illustrates that the haptic device is capable of rendering the required range of haptic feedback in all but one direction of pushing. However it was observed that the pushing force was above 5.62 N for only 23.57% of the procedure time for all subjects. Indicating our device's shortcoming in the requirement for actuation against pushing force is only for a fraction of the procedure time.

The frequency response of the device highlights the force bandwidth of the device. This shows the available range of frequencies at which a force can be transmitted to the user. It

was shown by Katsura *et al* that a narrow force bandwidth negatively impacts the system performace by slowing down the system convergence in a scenario requiring a step input, such as a sudden stop or collision [21]. Our device has 18.1 Hz and 5.7 Hz of force bandwidth in the translational and rotational DOFs. In the simulation a possible collision encounter (illustrated via a step input) would only be rendered through the translational feedback unit, for example hitting the abdominal wall. Our haptic device with 18.1 Hz of bandwidth in the translational DOF ensures a quick settling time of 0.12 seconds and overshoot-minimization. It was also noted that a settling time of 0.12 seconds was fairly short for a haptic device with significant damping. The high damping of the system is a desirable feature for impedance type haptic devices in order to increase the dynamic range of impedances [22]. As different soft tissue exhibit different impedances, this makes the device capable of rendering a wider range of soft tissue behavior. As long as the impedance controller compensates for the high damping at lower frequencies of motion, the obtained damping of the haptic device is a desirable characteristic.

The primary goal of the system characterization is to be able to identify the system behavior so it can be controlled. This experimentation will continue to further minmize the error between the experimental data and the estimated system models for more system transparency. The system will be re-evaluated with a human hand contact in the loop, which will alter system behavior as the human arm will introduce its own own impedance, contact forces and stiffness. All the identified parameters will then be used to develop controllers to compensate for inertia, high damping and frictional forces in the device. Karnopps friction model will be used to dynamically compensate for the friction in the system, in efforts to eventually minimze the systems output impedance.

V. Conclusion

In this paper we presented the design, development and evaluation of a novel haptic interface for the VTEST© simulator. Since NOTES procedures are different in their actuation and maneuvering requirement in comparison to other endoscopic procedures such as colonoscopy, the development of a custom haptic device was necessary. The hardware interface is designed to mimic the interactions a surgeon would have with a real patient in the OR during a NOTES surgery. The combined use of omni-directional friction rollers and a flexible drive shaft provides a robust decoupled haptic interface for transmitting force and torque to the user. The haptic device will be used with a simulation PC, which in real-time will render the simulated internal organs and be viewed by the trainee on an OR-like flat panel display.

References

[1] Mack MJ, "Minimally invasive and robotic surgery," *JAMA*, vol. 285, no. 5, pp. 568–572, Feb. 2001.

[2] D. Rattner and A. Kalloo, "ASGE/SAGES Working Group on Natural Orifice Translumenal Endoscopic Surgery: October 2005," *Surgical Endoscopy*, vol. 20, no. 2, pp. 329–333, Jan. 2006.

[3] R. D. Pai, D. G. Fong, M. E. Bundga, R. D. Odze, D. W. Rattner, and C. C. Thompson, "Transcolonic endoscopic cholecystectomy: a NOTES survival study in a porcine model (with video)," *Gastrointestinal Endoscopy*, vol. 64, no. 3, pp. 428–434, Sep. 2006.

[4] C. Rolanda, E. Lima, J. M. Pêgo, T. Henriques-Coelho, D. Silva, I. Moreira, G. Macedo, J. L. Carvalho, and J. Correia-Pinto, "Third-generation cholecystectomy by natural orifices: transgastric and transvesical combined approach (with video)," *Gastrointestinal Endoscopy*, vol. 65, no. 1, pp. 111–117, Jan. 2007.

[5] D. N. Moris, K. J. Bramis, E. I. Mantonakis, E. L. Papalampros, A. S. Petrou, and A. E. Papalampros, "Surgery via natural orifices in human beings: yesterday, today, tomorrow," *The American Journal of Surgery*, vol. 204, no. 1, pp. 93–102, Jul. 2012.

[6] R. Zorron, C. Palanivelu, M. P. Galvão Neto, A. Ramos, G. Salinas, J. Burghardt, L. DeCarli, L. Henrique Sousa, A. Forgione, R. Pugliese, A. J. Branco, T. S. Balashanmugan, C. Boza, F. Corcione, F. D'Ávila Avila, N. Arturo Gómez, P. A. Galvão Ribeiro, S. Martins, M. Filgueiras, K. Gellert, A. Wood Branco, W. Kondo, J. Inacio Sanseverino, J. A. G. de Sousa, L. Saavedra, E. Ramírez, J. Campos, K. Sivakumar, Pidigu Seshiyer Rajan, Priyadarshan Anand Jategaonkar, M. Ranagrajan, R. Parthasarathi, P. Senthilnathan, M. Prasad, D. Cuccurullo, and V. Müller, "International Multicenter Trial on Clinical Natural Orifice Surgery—NOTES IMTN Study: Preliminary Results of 362 Patients," *Surgical Innovation*, vol. 17, no. 2, pp. 142–158, Jun. 2010.

[7] R. Sotelo, R. de Andrade, G. Fernández, D. Ramirez, E. Di Grazia, O. Carmona, O. Moreira, A. Berger, M. Aron, M. M. Desai, and I. S. Gill, "NOTES Hybrid Transvaginal Radical Nephrectomy for Tumor: Stepwise Progression Toward a First Successful Clinical Case," *European Urology*, vol. 57, no. 1, pp. 138–144, Jan. 2010.

[8] K. Roberts, D. Solomon, R. Bell, and A. Duffy, "'Triangle of safety': anatomic considerations in transvaginal natural orifice surgery," *Surgical Endoscopy*, vol. 27, no. 8, pp. 2963–2965, May 2013.

[9] A. L. Trejos, S. Jayaraman, R. V. Patel, M. D. Naish, and C. M. Schlachta, "Force sensing in natural orifice transluminal endoscopic surgery," *Surgical endoscopy*, vol. 25, no. 1, pp. 186–192, 2011.

[10] E. Samur, L. Flaction, and H. Bleuler, "Design and Evaluation of a Novel Haptic Interface for Endoscopic Simulation," *IEEE Transactions on Haptics*, vol. 5, no. 4, pp. 301–311, 2012.

[11] K. Ikuta, K. Iritani, J. Fukuyama, and M. Takeichi, "Portable virtual endoscope system with force and visual display," Intelligent Robots and Systems, 2000. (IROS 2000). Proceedings. 2000 IEEE/RSJ International Conference on, vol. 1, pp. 720–726 vol.1, 2000.

[12] CAE Healthcare, http://www.caehealthcare.com/

[13] Simbionix USA Corporation, http://www.simbionix.com/

[14] A. Ferlitsch, P. Glauninger, A. Gupper, M. Schillinger, M. Haefner, A. Gangl, and R. Schoefl, "Evaluation of a virtual endoscopy simulator for training in gastrointestinal endoscopy," *Endoscopy*, vol. 34, no. 9, pp. 698–702, 2002.

[15] S. Dargar, G. Sankaranarayanan, and S. De, "The Use of Rotational Optical Encoders for Dial Sensing in the VirtualTranslumenal Endoscopic Surgical Trainer (VTEST©)," *Studies in health technology and informatics*, vol. 184, pp. 103–105, 2012.

[16] R. Ellis, O. Ismaeil, and M. Lipsett, "Design and evaluation of a high-performance haptic interface," *Robotica*, vol. 14, no. 3, pp. 321–328, 1996.

[17] V. Hayward and O. R. Astley, "Performance measures for haptic interfaces," in *Robotics Research*, Springer, 1996, pp. 195–206.

[18] S. A. Wall and W. Harwin, "A high bandwidth interface for haptic human computer interaction," *Mechatronics*, vol. 11, no. 4, pp. 371–387, Jun. 2001.

[19] E. Kunesch, F. Binkofski, and H.-J. Freund, "Invariant temporal characteristics of manipulative hand movements," *Experimental Brain Research*, vol. 78, no. 3, pp. 539–546, 1989.

[20] C. Brino, S. Dargar, G. Sankaranarayanan, K. Matthes, and S. De, "Haptic interactions during natural orifice translumenal endoscopic surgery," *Haptics Symposium (HAPTICS), 2014 IEEE*, pp. 617–622, Feb. 2014.

[21] S. Katsura, Y. Matsumoto, and K. Ohnishi, "Analysis and experimental validation of force bandwidth for force control," *Industrial Electronics, IEEE Transactions on*, vol. 53, no. 3, pp. 922–928, Jun. 2006.

[22] J. E. Colgate and J. M. Brown, "Factors affecting the Z-Width of a haptic display," *Robotics and Automation, 1994. Proceedings., 1994 IEEE International Conference on*, pp. 3205–3210 vol.4, May 1994.